Cell Transmembrane Receptors Determine Tissue Pattern Stability

Tilo Beyer[*,+]

Institute for Molecular and Clinical Immunology, Medical Faculty, Otto-von-Guericke-University, Leipziger Str. 44, 39120 Magdeburg, Germany

Michael Meyer-Hermann[*,‡]

Frankfurt Institute for Advanced Studies, Ruth-Moufang-Str. 1, 60438 Frankfurt Main, Germany

(Received 14 December 2007; published 30 September 2008)

The analysis of biological systems requires mathematical tools that represent their complexity from the molecular scale up to the tissue level. The formation of cell aggregates by chemotaxis is investigated using Delaunay object dynamics. It is found that when cells migrate fast such that the chemokine distribution is far from equilibrium, the details of the chemokine receptor dynamics can induce an *internalization driven instability* of cell aggregates. The instability occurs in a parameter regime relevant for lymphoid tissue and is similar to ectopic lymphoid structures.

DOI: 10.1103/PhysRevLett.101.148102 PACS numbers: 87.17.Jj, 87.17.Aa, 87.18.Hf

Experimental biology today gathers a large number of molecular and genetic data to understand processes in living systems. However, many questions of interest concern the level of cells, tissues or even larger structures. Mathematical models aim to translate molecular information into cellular behavior and function on various spatial and temporal scales. The present article follows this paradigm and focuses on the modeling of events from the molecular level up to small tissues.

Agent-based modeling allows to investigate macroscopic properties emerging from the collective behavior of individual units. A typical agent in biology is a single cell. Changes in the dynamics of the cell, e.g., surface properties and secreted molecules, can have effects on longer scales. Such long-scale effects are accessible with the Delaunay object dynamics method—a multiscale three-dimensional modeling framework [1,2]. The core component is an agent-based model of cells on top of a Delaunay triangulation [1,3,4]. It allows the engagement of biological systems where the information flow between the intracellular compartment and tissues becomes crucial. One well-known example where this information hierarchy plays a role is tissue organization by chemotaxis [5]. In the most simple case, chemotactic cues lead to the formation of aggregates. A more complex pattern is the spiral wave known for *Dictyostelium discoideum* [6,7].

It is known from *in vitro* experiments that chemokine receptors can be internalized [8]. The influence of the internalization dynamics on cell aggregate formation is investigated in this study. The cells are assumed to be leukocytes which are rather fast cells [9–11] such that the time scale of chemokine diffusion and cell movement are no longer well separated. Here it is shown that the details of the receptor dynamics of single cells have a significant impact on the cell behavior, even on the tissue level. Considering the seemingly simple system of a fixed number of cells that respond to a point source of chemokines results in a variety of patterns beyond a simple aggregation of the cells.

In the model cells are treated as soft elastic spheres in continuous three-dimensional space. Each cell can generate migration forces onto a not explicitly modeled extracellular matrix. Together with the strong friction in the tissue this gives rise to coupled Newtonian equations of motion in overdamped approximation [3,7]. The contact of cells is calculated on the basis of a Delaunay triangulation [1,3] which is updated according to the movement of the cells [4,12]. The mechanical parameters of cell migration have been fitted to match the speed distributions of highly motile immune cells in their natural environment [1].

In addition to mechanical forces generated by the cells, the dynamics of cell orientation, which determines the direction of the net force, is required. In the model the cell maintains its orientation during a persistence time T_p [11,13]. When the persistence time has passed the cell reorients according to the chemokine gradient. If the concentration difference between the front and the back of the cell is smaller than 2% [14], the cell performs a persistent random walk.

The impact of cell surface receptor dynamics on cell behavior is considered under the following assumptions (Fig. 1) [8]: (i) The signal for the cell is proportional to the ligand-induced phosphorylation of receptors. (ii) Phosphorylated receptors can be internalized. (iii) Internalized receptors are replaced on the surface by recycled or newly synthesized proteins. These processes are captured in the following set of equations:

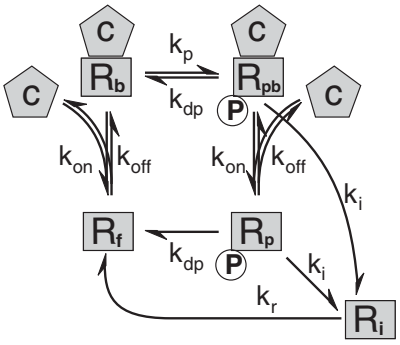

FIG. 1. Scheme of chemokine receptor dynamics. The receptor has five states: free (R_f), bound to the chemokine c (R_b), chemokine bound and phosphorylated (R_{pb}), ligand free but phosphorylated (R_p), and internalized (R_i). Only the phosphorylated forms (R_p, R_{pb}) are internalized and can be recycled back to the free receptor state R_f.

$$
\begin{aligned}
\dot{c} &= D\Delta c + Q - \kappa c - k_{\mathrm{on}}(R_f + R_p)c + k_{\mathrm{off}}(R_b + R_{pb}) \\
\dot{R}_f &= -\beta R_f - k_{\mathrm{on}} R_f c + k_{\mathrm{off}} R_b + k_{dp} R_p + \alpha + k_r R_i \\
\dot{R}_b &= -\beta R_b + k_{\mathrm{on}} R_f c - k_{\mathrm{off}} R_b - k_p R_b + k_{dp} R_{pb} \\
\dot{R}_{pb} &= -\beta R_{pb} + k_{\mathrm{on}} R_p c - k_{\mathrm{off}} R_{pb} + k_p R_b \\
&\quad - (k_{dp} + k_i) R_{pb} \\
\dot{R}_p &= -\beta R_p - k_{\mathrm{on}} R_p c + k_{\mathrm{off}} R_{pb} - (k_{dp} + k_i) R_p \\
\dot{R}_i &= k_i (R_p + R_{pb}) - k_r R_i
\end{aligned}
\tag{1}
$$

The chemokine c is secreted by a source with rate Q, is nonspecifically degraded with the rate constant κ, and diffuses with the diffusion coefficient D. The chemokine receptors on each cell can be in five states (Fig. 1): free (R_f), ligand-bound (R_b), ligand-bound and phosphorylated (R_{pb}), phosphorylated (R_p), and internalized (R_i). The internalized receptor cannot bind the chemokine and is recycled to the free surface receptor. The dynamics of the receptor influences the concentration profile of the chemokine c by sequestration. In addition the internalization of receptors with bound chemokine (R_{pb}) effectively degrades the chemokine. The chemokine receptor may have a constitutive turnover described by the ligand-independent degradation rate constant β and constant production α of the free receptor R_f. The parameters α and β are chosen such that, in the absence of the ligand, the amount of free receptor equals a given receptor expression $R_{\mathrm{tot}} = \alpha/\beta$. We would like to emphasize that some reaction rates are assumed to be independent of the receptor state, e.g., k_{on} and k_{off} do not depend on the phosphorylation of the receptor and k_{dp} and k_i are equal for bound and unbound chemokines.

In the model setup 5000 cells respond to the chemokine gradient generated by a static point source of strength Q in the center of the considered area. The parameters governing the receptor dynamics ($k_{[\cdot]}$, β), the chemokine characteristics (Q, D), or the cell migration (T_p) are varied relative to the reference parameter set in Table I.

TABLE I. Reference parameter set for the equation system [Eq. (1)] and experimental range with references. The parameters correspond to an unstable situation. A detailed discussion of the parameters can be found in [1].

Parameter	Unit	Value	Experimental range	Reference
κ	s^{-1}	2×10^{-4}	5×10^{-5}–7×10^{-4}	[15]
D	$\mu m^2\, s^{-1}$	10^1	10^1–10^3	[16]
Q	s^{-1}	2×10^3	10^3–10^4	[17]
β	s^{-1}	1×10^{-4}	1×10^{-5}–7×10^{-3}	[8]
R_{tot}		10^5	2×10^4–2×10^5	[18,19]
k_i	s^{-1}	5×10^{-4}	5×10^{-5}–3×10^{-2}	[8]
k_r	s^{-1}	2×10^{-4}	1×10^{-4}–7×10^{-3}	[8]
k_p	s^{-1}	1	10^{-1}–10^1	[20]
k_{dp}	s^{-1}	10^{-3}	10^{-3}–10^0	[20]
K_d	nM	3	0.2–5	[18,21]
k_{on}	$nM^{-1}\, s^{-1}$	10^7	2.5×10^5–10^8	[21]
k_{off}	s^{-1}	3×10^{-2}	10^{-4}–1	($= k_{\mathrm{on}} K_d$)
T_p	s	100	60–120	[11,13]

The internalization dynamics exhibits a regime which destabilizes the aggregate formation by chemotaxis. The cells aggregate for a relatively short time before they spread in the reaction volume and eventually form smaller aggregates distant to the center [22]. The major effect generating the instability is the fast cell migration compared to the diffusion of the chemokine. The internalization of the chemokine locally depletes the chemokine [22]. The gradient of the chemokine concentration is inverted at places with high cell density provided the chemokine receptors are in the corresponding states [Figs. 2(a) and 2(b)]. As cells can respond faster to the new gradient than the chemokine profile is restored by diffusion, the cells spread away from a temporarily formed aggregate.

The receptor dynamics of a single cell in the unstable aggregate is variable. Cells may exhibit rather stable or quasioscillating receptor states [Figs. 2(a) and 2(b)], or any mixture of these two extremes. The type of the receptor dynamics depends on the individual fate of a cell in the dynamically changing chemokine field.

To provide a measure for the instability the integral of a discrete Fourier transform (IFT) $\mathcal{F}(\cdot)$ of the second moment of the cell distribution [$\langle R^2 \rangle(t)$, Fig. 2(c)] was analyzed: $\mathrm{IFT} \overset{\mathrm{def}}{=} \int_0^\infty d\nu \mathcal{F}(\langle R^2 \rangle(t))(\nu)$.

The dependence of the cell aggregate stability on the chemokine receptor parameters is investigated. The cell aggregate becomes stable in cases that prevent the local depletion of the chemokine [Figs. 2(d)–2(g)]. This can be achieved by an increased source strength Q [Fig. 2(d)] that outcompetes the degradation of the chemokine by the cells or by an increased dephosphorylation of the receptor k_{dp} [Fig. 2(e)] and thereby a reduced internalization rate of ligand-receptor complexes. An increased diffusion coefficient D [Fig. 2(f)] can also compensate for the instability by allowing the chemokine to equilibrate faster such that

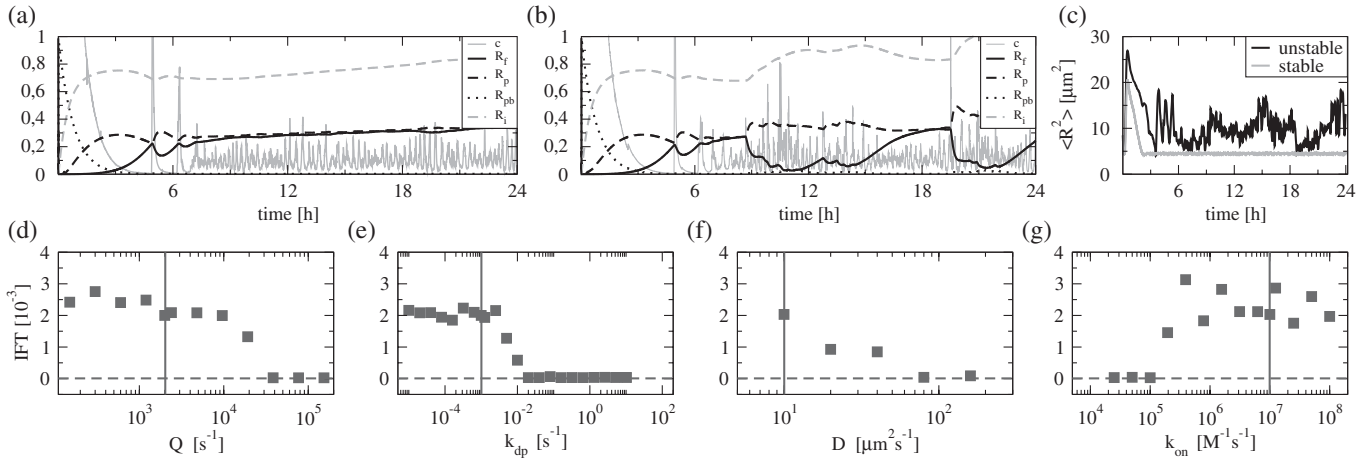

FIG. 2. Quantification of the internalization driven instability. (a),(b) Representative receptor kinetics of two cells are shown (reference model, parameters as in Table I, third column). The receptor states are normalized by R_{tot}. The concentration of the chemokine c along the cell migration path is shown in arbitrary units. Both cells start with identical kinetics—a result of the initial Poisson-distribution of the chemokine and not yet internalized receptors. Thereafter cells have an individual history with either almost monotone receptor kinetics (a) or quasioscillations (b) although both cells frequently encounter high and low chemokine concentrations. (c) Representative second moment $\langle R^2 \rangle(t)$ of the spatial cell distribution. One unstable ($Q = 2 \times 10^4$ s^{-1}) and one stable ($Q = 4 \times 10^4$ s^{-1}) case are shown. Initially the cells are distributed in a restricted volume and the chemokine is Poisson-distributed. The system equilibrates during the first 3 hours. The Fourier transform used for the phase diagrams (d)–(g) is taken for times $t > 12$ h. (d)–(g) Phase diagrams of cell aggregates in dependence on single parameters, where the reference value (Table I, third column) is marked in each diagram by a vertical line. All other parameters are set to their reference values (Table I, third column). Stable aggregates are characterized by IFT ≈ 0 (dashed line). A clear transition between stable and unstable aggregates is seen for the source strength Q (d) and the dephosphorylation rate k_{dp} (e). The transition is less strong for the diffusion coefficient D (f), and it occurs at very low binding rates k_{on} (g).

the chemokine distribution is dominated by diffusion rather than reaction in Eq. (1).

A change in the time-scale of receptor-ligand binding k_{on} (with constant K_d and adapted k_{off}) has no significant impact on the stability of the aggregate [Fig. 2(g)]. Only on-rates close to the lower physiological limit stabilize the aggregate. Then, internalization is effectively decreased by a low amount of chemokine-bound receptors.

In contrast to the other parameters the constitutive turnover of receptors modeled by α and β does not impact on cell aggregation for reasonable values.

The multiscale modeling framework presented in this study demonstrates that parameters of a complex biological system that act on a different scale than the particular problem under consideration can have significant impact on the results. This is a result based on the consideration of chemokine receptor dynamics for each cell giving rise to an internalization driven instability. Thus, it is the spatial discreteness of the cells that invalidates mean field approximations in this specific context.

Chemokine receptors can be targeted to different intracellular compartments after internalization. The internalized receptor can be either recycled and brought back to the surface without resynthesis or it can be degraded in lysosomes [8]. Experiments suggest that the major pathway is receptor recycling [23]. Therefore the parameters α and β are not strictly required which is in agreement with their lack of influence on the model results. Experimental data suggests that the majority of receptor dephosphorylation takes place in endosomes [23] implying that k_{dp} may not be required for the model [Eq. (1)]. However, this parameter influences the tissue level by determining the strength of ligand-induced internalization.

A challenge to our results is the fact that chemokines *in vivo* can induce chemotaxis only when bound to the surface of cells or the extracellular matrix [24]. Whether the receptor internalization or the uptake of the chemokine is modified under these conditions is not clear and requires corresponding experiments.

The described instability due to chemokine internalization may explain the shape of ectopic lymphoid follicles (Fig. 3). In the synovial tissue of rheumatoid arthritis patients so-called *dysmorphic follicles* [25] are often observed and represent a large variety of different follicle patterns. The less organized shape of follicles generated during certain diseases are presumably caused by a nonoptimal balance of the parameters of the chemokine-driven cell assembly, e.g., due to suboptimal production of chemokines at ectopic locations. Even though the large variety of observed shapes suggests that the fixed and stained sections exhibit snapshots of a highly dynamic follicle pattern, this cannot be deduced from single figures. It is well possible that the diversity of patterns corresponds to a diversity of static cell configurations.

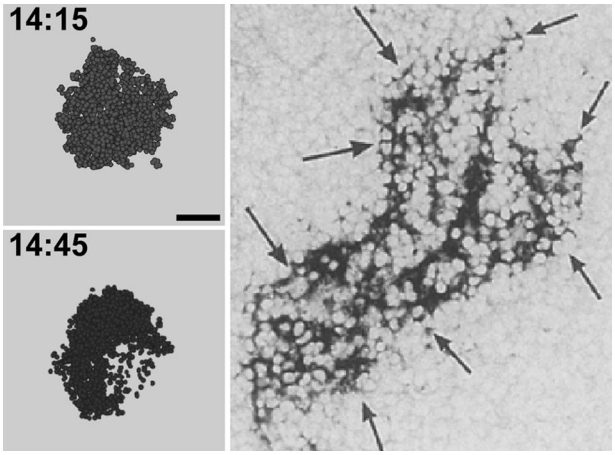

FIG. 3. Central sections of a cell aggregate (left panels) with a chemokine point source in the center of the section. Two sections at time HH:MM are shown to demonstrate the shape dynamics of the cell aggregate. The scale bar is 50 μm and the reference parameter set (Table I, third column) is used. The *in silico* sections are compared with the micrograph of an ectopic lymphoid follicle stained for follicular dendritic cells in the synovial tissue of a rheumatoid arthritis patient (right panel, reprint from [25] with the kind permission of Veit Krenn).

In conclusion multiscale modeling of a simple phenomenon like cell aggregation induced by a point source for a chemokine can reveal unexpected results within the known experimental range of parameters. The stability of the system is determined by the dynamics of receptor internalization in relation to chemokine diffusion. The patterns found for unstable cell aggregates resemble dysmorphic ectopic follicles in synovial tissue. Their pattern diversity is compatible with the interpretation that these emerge as a dynamic result of a mechanism which may be denoted as *internalization driven instability.*

More generally, it was demonstrated that the multiscale modeling approach allows to analyze the stability of the system once the biophysical parameters of a specific system are known. The expected properties of the tissue are not easily deduced from experimental molecular data, and thus the Delaunay object dynamics method can be used to complement the molecular profiles with their functional impact.

Tilo Beyer is supported by the FORSYS program of the German Ministry of Research and Education. FIAS is supported by the ALTANA AG. Michael Meyer-Hermann is supported by the EU-NEST project MAMOCELL within FP6.

*Corresponding authors.
[+]tilo.beyer@med.ovgu.de
[‡]M.Meyer-Hermann@fias.uni-frankfurt.de

[1] T. Beyer and M. Meyer-Hermann, Phys. Rev. E **76**, 021929 (2007).
[2] M. Meyer-Hermann, Curr. Topics Dev. Biol. **81**, 373 (2008).
[3] G. Schaller and M. Meyer-Hermann, Phys. Rev. E **71**, 051910 (2005).
[4] T. Beyer, G. Schaller, A. Deutsch, and M. Meyer-Hermann, Comput. Phys. Commun. **172**, 86 (2005).
[5] J. G. Cyster, Science **286**, 2098 (1999).
[6] K. J. Tomchik and P. N. Devreotes, Science **212**, 443 (1981).
[7] E. Palsson and H. G. Othmer, Proc. Natl. Acad. Sci. U.S.A. **97**, 10 448 (2000).
[8] N. F. Neel, E. Schutyser, J. Sai, G. H. Fan, and A. Richmond, Cytokine Growth Factor Rev. **16**, 637 (2005).
[9] P. P. H. de Bruyn, Anat. Rec. **93**, 295 (1945).
[10] J. Murray, H. Vawter-Hugart, E. Voss, and D. R. Soll, Cell Motil. Cytoskeleton **22**, 211 (1992).
[11] S. H. Wei, I. Parker, M. J. Miller, and M. D. Cahalan, Immuno. Rev. **195**, 136 (2003).
[12] G. Schaller and M. Meyer-Hermann, Comput. Phys. Commun. **162**, 9 (2004).
[13] E. Albrecht and H. R. Petty, Proc. Natl. Acad. Sci. U.S.A. **95**, 5039 (1998).
[14] C. A. Parent and P. N. Devreotes, Science **284**, 765 (1999).
[15] A. Bar-Even, J. Paulsson, N. Maheshri, M. Carmi, E. O'Shea, Y. Pilpel, and N. Barkai, Nat. Genet. **38**, 636 (2006).
[16] G. J. Randolph, V. Angeli, and M. A. Swartz, Nat. Rev. Immunol. **5**, 617 (2005).
[17] J. L. Vissers, F. C. Hartgers, E. Lindhout, C. G. Figdor, and G. J. Adema, Euro. J. Immunol. **31**, 1544 (2001).
[18] K. Willimann, D. F. Legler, M. Loetscher, R. S. Roos, M. B. Delgado, I. Clark-Lewis, M. Baggiolini, and B. Moser, Euro. J. Immunol. **28**, 2025 (1998).
[19] T. Okada, V. N. Ngo, E. H. Ekland, R. Forster, M. Lipp, D. R. Littman, and J. G. Cyster, J. Exp. Med. **196**, 65 (2002).
[20] T. J. Lukas, Biophys. J. **87**, 1406 (2004).
[21] A. J. Pelletier, L. J. van der Laan, P. Hildbrand, M. A. Siani, D. A. Thompson, P. E. Dawson, B. E. Torbett, and D. R. Salomon, Blood **96**, 2682 (2000).
[22] See EPAPS Document No. E-PRLTAO-101-026838 for two movies showing sections of an unstable cell aggregate and the corresponding chemokine distribution with color-coded concentrations increasing from blue to red. For more information on EPAPS, see http://www.aip.org/pubservs/epaps.html.
[23] A. Mueller, E. Kelly, and P. G. Strange, Blood **99**, 785 (2002).
[24] A. E. Proudfoot, T. M. Handel, Z. Johnson, E. K. Lau, P. LiWang, I. Clark-Lewis, F. Borlat, T. N. Wells, and M. H. Kosco-Vilbois, Proc. Natl. Acad. Sci. U.S.A. **100**, 1885 (2003).
[25] V. Krenn, N. Schalhorn, A. Greiner, R. Molitoris, A. Konig, F. Gohlke, and H. K. Muller-Hermelink, Rheumatology Int. **15**, 239 (1996).